



Supporting Online Material for

The Sand Seas of Titan: Cassini RADAR Observations of Longitudinal Dunes

R. D. Lorenz,* S. Wall, J. Radebaugh, G. Boubin, E. Reffet, M. Janssen, E. Stofan, R. Lopes, R. Kirk, C. Elachi, J. Lunine, K. Mitchell, F. Paganelli, L. Soderblom, C. Wood, L. Wye, H. Zebker, Y. Anderson, S. Ostro, M. Allison, R. Boehmer, P. Callahan, P. Encrenaz, G. G. Ori, G. Francescetti, Y. Gim, G. Hamilton, S. Hensley, W. Johnson, K. Kelleher, D. Muhleman, G. Picardi, F. Posa, L. Roth, R. Seu, S. Shaffer, B. Stiles, S. Vetrella, E. Flamini, R. West

*To whom correspondence should be addressed. E-mail: rlorenz@lpl.arizona.edu

Published 5 May 2006, *Science* **312**, 724 (2006)
DOI: 10.1126/science.1123257

This PDF file includes:

Materials and Methods
SOM Text
Figs. S1 and S2
References

Observation Details

The Cassini RADAR instrument is described in detail in (S1). It transmits and receives 2cm radiation in the same linear polarization : the projection of this direction onto the ground is such that the images are essentially of HH backscatter. The incidence angle at the center of the image varies throughout the pass from about 18 to 23 degrees. The antenna is fed with a set of waveguides to yield a fan-shaped beam 5.75° wide, which yields a useable imaging swath whose width depends on altitude.

The T8 encounter had closest approach to Titan (1353km altitude) on 27th October 2005 : the useable swath width varies between ~200km and 450km. SAR imaging was performed from 20 minutes prior to closest approach to 18 minutes after, yielding a swath some 5000km long. Near closest approach the azimuth resolution (left-right in Figs 1 and 3) was ~300m, while the range resolution was ~450m. At longer ranges (at the beginning and end of the observation) the resolution degraded to ~1km in each case.

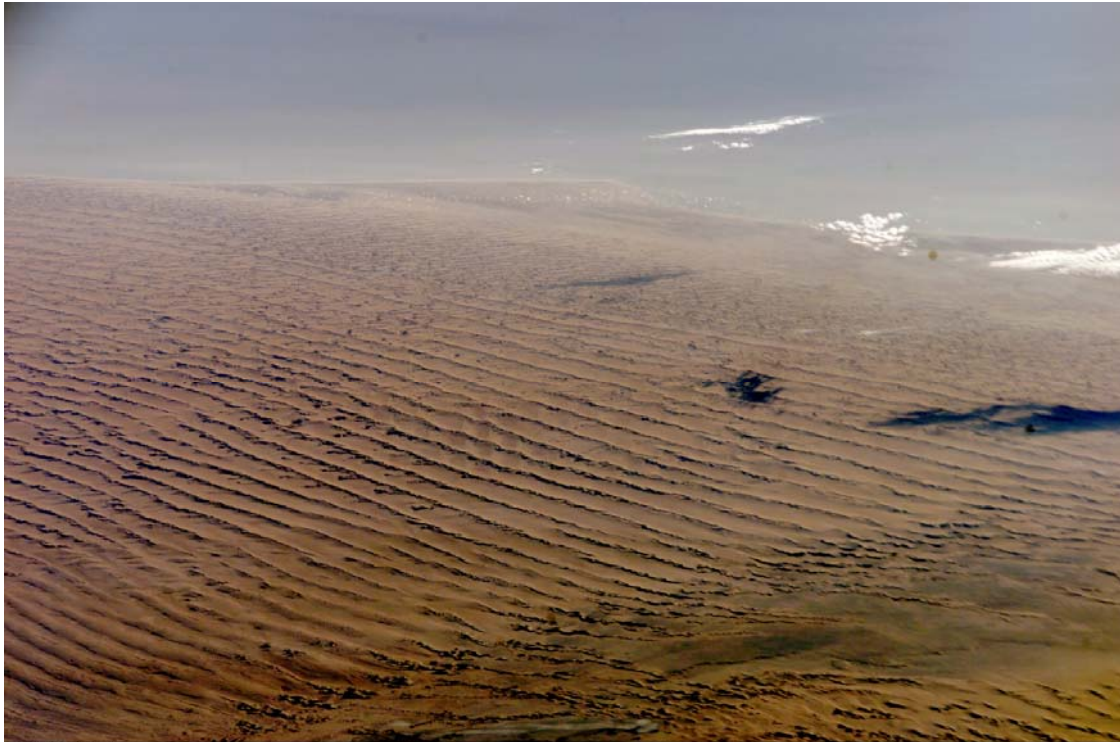
Radar Appearance of Dunes

Radar images indicate backscatter – at the incidence angles typical for SAR, a bright feature usually implies one or more of the following factors : a rough surface at wavelength scales or higher, a surface composed of high dielectric constant (typically, high density) materials, or a surface tilted towards the radar. In low-absorption materials (very dry and/or very cold) subsurface reflection or scattering may add to the measured reflectivity.

Sand dunes are typically radar-dark (compared to the underlying material), since sand is typically smooth at radar wavelengths of several cm, and it has a lower dielectric constant than competent rock. The exception is where faces of the dune are oriented towards the radar, resulting in a bright and sometimes dazzling glint. The superposition of smaller duneforms in compound dunes, or the presence of ripples may affect the appearance of dunes to Radar. Fig. S1 shows a radar image of a terrestrial sand sea – the similarities with the Titan images are obvious. Fig S2 shows an optical image of the same region, albeit with a different viewing geometry. In this case (the Namib desert) the longitudinal dunes are formed by a seasonally-switching wind direction (S2).



Fig. S1. A 100x70km segment of a SAR image of the Namib desert on Earth (24°S, 15°E), acquired by the Shuttle Imaging Radar (SIR-C/X-SAR) mission in 1994. This image is at L-band (24cm) wavelength, HH polarization. North is towards bottom left ; radar illumination is from above. The bright region at bottom right is the Atlantic Ocean – the pattern of large longitudinal dunes that dominates the image is broken at the shore, and at the mouth of the Tschauibrivier (top right) which no longer reaches the sea. Bright glints are widespread in this region, due to numerous facets in star-shaped dunes. The mean transport direction is from right to left.
SIR-C Datatake 58.40 processing run PR44419. SIR-C data obtained from the EROS data center <http://edc.usgs.gov/>



S107E05380

Fig. S2 Handheld digital camera image (roll E, frame 5380) acquired from the Space Shuttle mission STS-107 at 283km altitude with a 400mm lens of the Namib desert just to the North of figure in S1 (in this case looking south-west).. A section from the lower left is shown in figure 2b. Image courtesy of Earth Sciences and Image Analysis Laboratory, NASA Johnson Space Center <http://eol.jsc.nasa.gov>

Transport Timescales

One expression for the transport rate q for sand (3,13,S3) is given by $q=2.6(\rho_a/g)(V_*-V_{*t})(V_*+V_{*t})^2$, where g is local gravity and ρ_a the atmospheric density. The time to transport a feature of height h with material density ρ by a distance D is, neglecting factors of order unity, $\sim hD\rho/q$. Assuming a threshold speed of 2 cms^{-1} and a freestream wind of 0.5 ms^{-1} , the time to assemble a uniform sheet of sand into the observed dunes ($h\sim 50 \text{ m}$, $D\sim 1000 \text{ m}$) is of the order of several kyr. Even quite large dunes can form in 1-2 kyr on Earth (S4). To transport sand over global scales ($D\sim 1000 \text{ km}$), creating the low-latitude belt of dune features with material from mid-latitudes, requires $\sim 1 \text{ Myr}$. These estimates must be considered highly uncertain (by an order of magnitude or more : the cubic dependence of transport rate means that transport is dominated by the high-speed tail of the windspeed probability distribution, about which little information exists for Titan) but serve to provide at least a crude minimum timescale. The timescale is a lower limit since sand may be removed from as well as supplied to a growing dune, such that the net accumulation is lower than indicated above.

It is interesting that these timescales are broadly comparable with those on Earth – the ease of transporting material compensates for the low windspeeds, such that the net rates are similar.

The dune formation timescale is long compared to the tidal cycle (Titan's day and orbital period, namely 15.95 Earth days) and to the seasonal cycle (29.5 Earth years) over which the winds are likely to vary. Thus the dunes observed in October 2005 must reflect wind patterns averaged over these diurnal and annual periods.

References

S1. Elachi, C.; Allison, M. D.; Borgarelli, L.; Encrenaz, P.; Im, E.; Janssen, M. A.; Johnson, W. T. K.; Kirk, R. L.; Lorenz, R. D.; Lunine, J. I.; Muhleman, D. O.; Ostro, S. J.; Picardi, G.; Posa, F.; Rapley, C. G.; Roth, L. E.; Seu, R.; Soderblom, L. A.; Vetrilla, S.; Wall, S. D.; Wood, C. A.; Zebker, H. A., RADAR : The Cassini Titan Radar Mapper, Space Science Reviews, Volume 115, Issue 1-4, pp. 71-110, 2004

S2. Breed, C. S., S. G. Fryberger, S. Andrews, C. McCauley, F. Lennartz, D. Gebel and K. Horstman, Regional Studies of Sand Seas, Using Landsat (ERTS) Imagery, pp.305-397 in E. D. McKee (ed) A Study of Global Sand Seas, Geological Survey Professional Paper 1052, U.S. Government Printing Office, Washington D.C., 1979

S3. White, B., Soil Transport by Winds on Mars, Journal of Geophysical Research, 84, 4643-4651, 1979

S4. Lancaster, N. et al., Late Pleistocene and Holocene Dune activity and wind regimes in the western Sahara of Mauritania, Geology, 30, 991-994, 2002.